

Apparent Clustering and Apparent Background Earthquakes Biased by Undetected Seismicity

Didier Sornette

Department of Earth and Space Sciences, and Institute of Geophysics and Planetary Physics, University of California, Los Angeles, USA and Laboratoire de Physique de la Matière Condensée, CNRS UMR6622, Université de Nice-Sophia Antipolis, France

Maximilian J. Werner

Department of Earth and Space Sciences, and Institute of Geophysics and Planetary Physics, University of California, Los Angeles, USA

Abstract.

In models of triggered seismicity and in their inversion with empirical data, the detection threshold m_d is commonly equated to the magnitude m_0 of the smallest triggering earthquake. This unjustified assumption neglects the possibility of shocks below the detection threshold triggering observable events. We introduce a formalism that distinguishes between the detection threshold m_d and the minimum triggering earthquake $m_0 \leq m_d$. By considering the branching structure of one complete cascade of triggered events, we derive the apparent branching ratio n_a (which is the apparent fraction of aftershocks in a given catalog) and the apparent background source S_a that are observed when only the structure above the detection threshold m_d is known due to the presence of smaller undetected events that are capable of triggering larger events. If earthquake triggering is controlled in large part by the smallest magnitudes as several recent analyses have shown, this implies that previous estimates of the clustering parameters may significantly underestimate the true values: for instance, an observed fraction of 55% of aftershocks is renormalized into a true value of 75% of triggered events.

1. Introduction

There are numerous evidences that a seismic event can have a significant effect on the pattern of subsequent seismicity, most obvious in aftershocks of large events. More recently has emerged an important extension of the concept of earthquake interactions in the concept of triggered seismicity, in which the usual distinction, that foreshocks are precursors of larger mainshocks which in turn trigger smaller aftershocks, becomes blurred: a parsimonious and efficient description of seismicity does not seem to require the division between foreshocks, mainshocks and aftershocks, which appear indistinguishable from the point of view of many of their physical and statistical properties [Helmstetter and Sornette, 2003a]. An important logical consequence is that cascades of triggered seismicity (“aftershocks,” “aftershocks” of “aftershocks,” ...) may play an important role in the overall seismicity budget [Helmstetter and Sornette, 2003b; Felzer et al., 2002].

There is thus a growing interest in phenomenological models of triggered seismicity, which use the Omori law as the best coarse-grained proxy for modeling the complex and multi-faceted interactions between earthquakes, together with the other most solid stylized facts of seismicity (clustering in space, the Gutenberg-Richter (GR) earthquake size distribution and an aftershock productivity law). This class of ETAS (Epidemic-Type Aftershock Sequences) models introduced by Ogata [1988] and Kagan and Knopoff [1981] offers a parsimonious approach replacing the classification of foreshocks, mainshocks and aftershocks by the concept of earthquake triggering: earthquakes may trigger

other earthquakes through a variety of physical mechanisms but the effective laws do not allow the identification of a particular mechanism.

The questions suggested by this approach include: 1) what is the fraction of triggered versus uncorrelated earthquakes (which is linked to the problem of clustering)? How can one use this modeling approach to forecast future seismicity? What are the limits of predictability and how are they sensitive to catalog completeness and type of tectonic deformation? In general, to attack any such question, one needs in one way or another to estimate some key parameters of the models of triggered seismicity.

The royal path is in principle to use the maximum likelihood method to estimate the parameters of the considered model from a catalog of seismicity (time, location and magnitude) (see for instance Ogata [1988] and Kagan [1991]). The calculation of the likelihood function requires evaluating the theoretical rate of seismicity at time t induced by all past events at times $t_i < t$. The maximization of the likelihood with respect to the parameters of the model, given the data, then provides an estimate of the parameters. All previous studies have considered that small earthquakes, below the detection threshold, are negligible. Thus, the rate of seismicity is calculated as if triggered only by earthquakes above the detection threshold. However, this method is not correct because it does not take into account events below the detection threshold, which may have an important role in the triggering of seismicity. Indeed, small earthquakes have a significant contribution in earthquake triggering because they are much more numerous than larger earthquakes (Helmstetter [2003]; Felzer et al. [2002]; Helmstetter et al. [2004]). This can simply be seen from the competition between the productivity law $\sim 10^{\alpha M}$ giving the number of events triggered by a mainshock of magnitude M and the relative abundance $\sim 10^{-bM}$ of such mainshocks given by the Gutenberg-Richter law: the contribution of earthquakes of magnitude M to the overall seismic rate is thus

$\sim 10^{-(b-\alpha)M}$, which is dominated by small M 's for $\alpha < b$ [Helmstetter, 2003] or equally contributed by each magnitude class for $\alpha = b$ (Felzer *et al.* [2002]; Helmstetter *et al.* [2004]). Therefore, one needs to take into account small events that are not observed in order to calibrate correctly models of seismicity and obtain reliable answers to our questions stated above. This is an essential bottleneck for the development of earthquake forecasts based on such models.

The purpose of this note is to present a general theoretical treatment of the impact of unobserved seismicity within the framework of models of triggered seismicity. We show by analyzing the branching structure of a complete cascade (cluster) triggered by an independent background event that the unobserved seismicity has the effect of decreasing the real branching ratio n and of increasing the number of independent background events S into apparent quantities n_a and S_a . This bias may be very significant. We therefore claim that previous work should be reanalyzed from the new perspective of our approach. This leads also to important consequences for the methods presently used to forecast future seismicity based only on incomplete catalogs.

2. The ETAS model and the smallest triggering earthquake

2.1. Definition of the ETAS model

To make this discussion precise, let us consider the epidemic-type aftershock sequence (ETAS) model, in which any earthquake may trigger other earthquakes, which in turn may trigger more, and so on. Introduced in slightly different forms by Kagan and Knopoff [1981] and Ogata [1988], the model describes statistically the spatio-temporal clustering of seismicity.

The triggering process may be caused by various mechanisms that either compete or combine, such as pore-pressure changes due to pore-fluid flows coupled with stress variations, slow redistribution of stress by aseismic creep, rate-and-state dependent friction within faults, coupling between the viscoelastic lower crust and the brittle upper crust, stress-assisted micro-crack corrosion, and more. The ETAS formulation amounts to a two-scale description: these above physical processes controlling earthquake interactions enter in the determination of effective triggering laws in a first step and the overall seismicity is then seen to result from the cascade of triggering of events triggering other events triggering other events and so on [Helmstetter and Sornette, 2002].

The ETAS model consists of three assumed laws about the nature of seismicity viewed as a marked point-process. We restrict this study to the temporal domain only, summing over the whole spatial domain of interest. First, the magnitude of any earthquake, regardless of time, location, or magnitude of the mother shock, is drawn randomly from the exponential Gutenberg-Richter (GR) law. Its normalized probability density function (pdf) is expressed as

$$P(m) = \frac{b \ln(10) 10^{-bm}}{10^{-bm_0} - 10^{-bm_{max}}}, m_0 \leq m \leq m_{max}, \quad (1)$$

where the exponent b is typically close to one, and the cut-offs m_0 and m_{max} serve to normalize the pdf. The upper cut-off m_{max} is introduced to avoid unphysical, infinitely large earthquakes. Its value was estimated to be in the range 8–9.5 [Kagan, 1999]. As the impact of a finite m_{max} is quite weak in the calculations below, replacing the abrupt cut-off m_{max} by a smooth taper would introduce negligible corrections to our results.

Second, the model assumes that direct aftershocks are distributed in time according to the modified “direct” Omori law (see Utsu *et al.* [1995] and references therein). Assuming

$\theta > 0$, the normalized pdf of the Omori law can be written as

$$\Psi(t) = \frac{\theta c^\theta}{(t+c)^{1+\theta}}. \quad (2)$$

Third, the number of direct aftershocks of an event of magnitude m is assumed to follow the productivity law:

$$\rho(m) = k 10^{\alpha(m-m_0)}, m_0 \leq m \leq m_{max}. \quad (3)$$

Note that the productivity law (3) is zero below the cut-off m_0 , i.e. earthquakes smaller than m_0 do not trigger other earthquakes, as is typically assumed in studies using the ETAS model. The existence of the small magnitude cut-off m_0 is necessary to ensure the convergence of these types of models of triggered seismicity (in statistical physics of phase transitions and in particle physics, this is called an “ultra-violet” cut-off which is often necessary to make the theory convergent). In a closely related paper, Sornette and Werner [2004] showed that the existence of the cut-off m_0 has observable consequences which constrain its physical value.

The key parameter of the ETAS model is defined as the number n of direct aftershocks per earthquake, averaged over all magnitudes. Here, we must distinguish between the two cases $\alpha = b$ and $\alpha \neq b$:

$$\begin{aligned} n &\equiv \int_{m_0}^{m_{max}} P(m) \rho(m) dm \\ &= \frac{kb}{b-\alpha} \left(\frac{1 - 10^{-(b-\alpha)(m_{max}-m_0)}}{1 - 10^{-b(m_{max}-m_0)}} \right), \end{aligned} \quad (4)$$

for the general case $\alpha \neq b$. The special case $\alpha = b$ gives

$$n = \frac{kb \ln(10)(m_{max} - m_0)}{1 - 10^{-b(m_{max} - m_0)}} \quad (5)$$

Three regimes can be distinguished based on the value of n . The case $n < 1$ corresponds to the subcritical, stationary regime, where aftershock sequences die out with probability one. The case $n > 1$ describes unbounded, exponentially growing seismicity [Helmstetter and Sornette, 2002]. In addition, the case $b < \alpha$ leads to explosive seismicity with finite time singularities [Sornette and Helmstetter, 2002]. The critical case $n = 1$ separates the two regimes $n < 1$ and $n > 1$. Helmstetter and Sornette [2003b] showed that the branching ratio n is also equal to the fraction of triggered events in a seismic catalog.

The fact that we use the same value for the productivity cut-off and the Gutenberg-Richter (GR) cut-off is not a restriction as long as the real cut-off for the Gutenberg-Richter law is smaller than or equal to the cut-off for the productivity law. In that case, truncating the GR law at the productivity cut-off just means that all smaller earthquakes, which do not trigger any events, do not participate in the cascade of triggered events. This should not be confused with the standard incorrect procedure in many previous studies of triggered seismicity of simply replacing the GR and productivity cut-off m_0 with the detection threshold m_d in equations (1) and (3) (see, for example, Ogata [1988]; Kagan [1991]; Ogata [1998]; Console *et al.* [2003]; Zhuang *et al.* [2004]). The assumption that $m_d = m_0$ may lead to a bias in the estimated parameters.

Without loss of generality, we consider one independent branch (cluster or cascade of aftershocks set off by a background event) of the ETAS model. Let thus an independent background event of magnitude M_1 occur at some origin

of time. The mainshock will trigger direct aftershocks according to the productivity law (3). Each of the direct aftershocks will trigger their own aftershocks, which in turn produce their own, and so on. Averaged over all magnitudes, an aftershock produces n direct offsprings according to (4). Thus, in infinite time, we can write the average of the total number N_{total} of direct and indirect aftershocks of the initial mainshock as an infinite sum over terms of (3) multiplied by n to the power of the generation [Helmstetter and Sornette, 2003b], which can be expressed for $n < 1$ as:

$$\begin{aligned} N_{total} &= \rho(M_1) + \rho(M_1)n + \rho(M_1)n^2 + \dots \\ &= \frac{k10^{\alpha(M_1-m_0)}}{1-n} \end{aligned} \quad (6)$$

However, since we can only detect events above the detection threshold m_d , the total number of observed aftershocks N_{obs} of the sequence is simply N_{total} multiplied by the fraction of events above the detection threshold, given by

$$f_{obs} = \frac{10^{b(m_{max}-m_d)} - 1}{10^{b(m_{max}-m_0)} - 1} \quad (7)$$

according to the GR distribution. The observed number of events in the sequence is therefore

$$\begin{aligned} N_{obs} &= N_{total}f_{obs} \\ &= \frac{k10^{\alpha(M_1-m_0)}}{1-n} \left(\frac{10^{b(m_{max}-m_d)} - 1}{10^{b(m_{max}-m_0)} - 1} \right). \end{aligned} \quad (8)$$

Equation (8) predicts the average observed number of direct and indirect aftershocks of a mainshock of magnitude $M_1 > m_d$. Sornette and Werner [2004] showed that m_0 may be estimated using fits of N_{obs} given by (8) to observed aftershock sequences and B ath's law. The essential parameter needed to constrain m_0 is the branching ratio n . As we demonstrate below, typical estimates of n in the literature obtained from a catalog neglect undetected seismicity and therefore cannot be used directly to constrain m_0 .

Naturally, there is no justification for assuming that m_d should equal m_0 , as is done routinely in inversions of catalogs for the parameters of the ETAS model (see, for example, Ogata [1988]; Kagan [1991]; Ogata [1998]; Console *et al.* [2003]; Zhuang *et al.* [2004]). First, detection thresholds change over time as instruments and network coverage become better, while the physical mechanisms in the Earth presumably remain the same. No significant deviation from the Gutenberg-Richter distribution or the productivity law has been recorded as the detection threshold m_d decreased over time. Second, studies of earthquake occurrence at small magnitude levels below the regional network cut-offs show that earthquakes follow the same Gutenberg-Richter law (for a recent study of mining-induced seismicity, see, for example, Sellers *et al.* [2003]), while acoustic emission experiments have shown the relevance of the Omori law at small scales (see, for instance Nechad *et al.* [2004] and references therein). Within the assumption of self-similarity, i.e. a continuation of the GR and productivity laws down to a cut-off, evidence thus points towards a magnitude of the smallest triggering earthquake and a Gutenberg-Richter cut-off that lie below the detection threshold and are thus not directly observable.

2.2. Two interpretations of the ETAS model

The ETAS model may be viewed in two mathematically equivalent but interpretationally different ways. In this section, we develop both views to underline that our results apply in both cases and to stress the equivalence of these two views. The first describes the model as a simple branching model without loops: The independent background events,

due to tectonic loading, may each independently trigger direct aftershocks, each of which may in turn trigger secondary shocks, which in turn may trigger more. Because every triggered event, excluding of course the non-triggered background events, has exactly one mainshock (mother), but the mother may have many direct aftershocks (children), the model can be thought of as a simple branching model without loops. The background events are assumed to be a stationary Poisson process with a constant rate. The rate of the aftershocks of a background event is a non-stationary Poisson process that is updated every time another aftershock occurs until the cascade dies out. The intensity is thus conditioned on the specific history of earthquakes. The expectation of the conditional intensity is an average over an ensemble of histories. The predicted number of aftershocks of an independent background event of magnitude M_1 as in expression (8) is thus averaged over the ensemble of possible realizations of the aftershock sequence, and it is also averaged over all possible magnitudes of the aftershocks. The branching ratio n is therefore an average not only over magnitudes but also over an ensemble of realizations of the non-stationary Poisson process. The model thus consists of statistically independent Poisson clusters of events, which are, however, dependent within one cluster.

The second view of the ETAS model does not allow a unique identification of the mother or trigger of an earthquake. Rather, each aftershock was triggered collectively by all previous earthquakes, each of which contributes a weight determined by the magnitude-dependent productivity law $\rho(m)$ that decays in time according to the Omori law $\psi(t)$ and in space according to a spatial function $R(r)$, often chosen to be an exponential or a power law centered on the event. The instantaneous conditional intensity rate at some time t at location r is given by

$$\lambda(t, r) = \mu + \sum_{i|t_i < t} \rho(m_i)\psi(t - t_i)R(r - r_i) \quad (9)$$

where the sum runs over all previous events i with magnitude m_i at time t_i at location r_i . Thus the triggering contribution of a previous event to a later event at time t is given by its own weight (its specific entry in the sum) divided by the total seismicity rate, including the background rate. A non-zero background rate then contributes evenly to all events and corresponds to an omnipresent loading contribution. In this way, earthquakes are seen to be the result of all previous activity including the background rate. This corresponds to a branching model in which every earthquake links to all subsequent earthquakes weighted according to the contribution to triggering. A branching ratio can then be interpreted as a contribution of a past earthquake to a future earthquake, averaged over an ensemble of realizations and all magnitudes. This second view becomes the only possible one for nonlinear models whose triggering functions depend nonlinearly on previous events (see e.g. the recently introduced multi-fractal earthquake triggering model by Ouillon and Sornette [2004] and references therein).

These two views are equivalent because the linear formulation of the seismic rate of the ETAS model together with the exponential Poisson process ensures that the statistical properties of the resulting earthquake catalogs are the same. The linear sum over the individual contributions and the Poisson process formulation are the key ingredients that allow the model to be viewed as a simple branching model.

This duality of thinking about the ETAS model is reflected in the existence of two simulation codes in the community, each inspired by one of the two views. A program written by K. Felzer and Y. Gu (personal communication) calculates the background events as a stationary Poisson

process and then simulates each cascade independently of the other branches as a non-stationary process. The second code by *Ogata* [1998], on the other hand, calculates the overall seismicity at each point in time by summing over all previous activity. The latter code is significantly slower because the independence between cascades is not used, and the entire catalog is modeled as the sum of a stationary and a non-stationary process. Despite the different approach, both resulting earthquake catalogs share the same statistical properties and are thus equally acceptable. In the interpretation of the model as a simple branching model, the parameter n defined in (4) would correspond to a branching ratio, while the view that aftershocks are triggered collectively by all previous earthquakes and the background rate would interpret n as an average contribution of a single earthquake on future earthquakes. The important point is that the statistical properties are the same.

While the simulation or forward problem is straightforward when adopting the view of the ETAS model as a branching model with one assigned trigger for any aftershock, the inverse problem of reconstructing the branching structure from a given catalog can at best be probabilistic. Because aftershocks of one mother cannot be distinguished from those of another mother except by spatio-temporal distance, we have no way of choosing which previous earthquake triggered a particular event, or whether it is a background event. Rather, we must resort to calculating the probability of an event at time t to be triggered by any previous event according to the contribution that the previous event has at time t compared to the overall intensity at time t . This probability is of course equal to the weight or triggering contribution that a previous event has on a subsequent event when adopting the collective-triggering view. However, the interpretation remains different since the probability specifies a unique mother in a fraction of many realizations.

Having determined from catalogs a branching structure weighted according to the probability of triggering, one may of course choose to always pick as source of an event the most probable contributor, be that a previous event or the background rate. Another option is to choose randomly according to the probability distribution and thus reconstruct one possible branching structure among the ensemble of many other possible ones. The latter approach has been used by *Zhuang et al.* [2004] and labeled stochastic reconstruction.

The key point is that equating the detection threshold with the smallest triggering earthquake will most likely lead to a bias in the recovered parameters of a maximum likelihood analysis as performed by *Zhuang et al.* [2004] and in many other studies. Therefore, the weights or probabilities of previous events triggering subsequent events were calculated from biased parameters.

In the following, we show that the branching ratio and the background source events are significantly biased when they are estimated from the apparent branching structure observed above the detection threshold m_d instead of the complete tree structure down to m_0 . We adopt the view of the simple branching model to make the derivations more illuminating but all results can be reinterpreted as contributions in the collective-triggering view.

3. The Apparent Branching Structure of the ETAS Model

3.1. The apparent branching ratio n_a

Seismic catalogs are usually considered complete above a threshold m_d , which varies as a function of technology and location. For instance, $m_d \approx 2$ for modern Southern California catalogs (and for earthquakes not too close in time to a large mainshock [*Kagan*, 2003]). The analysis of the statistics of the Omori and inverse Omori laws for earthquakes of

magnitude down to 3 (*Helmstetter* [2003]; *Helmstetter and Sornette* [2003a]) suggests that m_0 is smaller than the completeness magnitude m_d and is thus not directly observable. Thus, m_0 is the size of the smallest triggering earthquake, which most likely differs significantly in size from the current detection threshold m_d . By considering the branching structure of the model, we derive the apparent branching ratio and the apparent background source that are found if only the observed (detected) part of the ETAS model is analyzed.

As stated above, the ETAS model consists of statistically independent Poisson-distributed clusters. Within each cluster, each shock has exactly one trigger, apart from the initial background event (mainshock) that sets off the cascade. We restrict this study to the case $n < 1$ for mathematical convenience and because this range of branching ratios gives rise to statistically stationary seismic sequences.

Since aftershock clusters are independent of each other, averages of one cluster are equal to ensemble averages, as nothing but the inherent stochasticity of the model determines the properties of the clusters. One cluster consists of one independent background event (source) and its direct and indirect aftershocks. However, if not all events of the sequence are detected, then there will appear to be less direct (and indirect) aftershocks, i.e. the branching ratio will appear different. Furthermore, some observed events will be triggered by mother-earthquakes below the detection threshold, resulting in apparently independent background events.

We will refer to the observed branching structure above the detection threshold as the apparent structure. As a useful visualization of the effect of the detection threshold on the branching structure, one can think of the branching structure as a mountain range that is submerged to some fraction of its height in water (see Figure 1). The height of each mountain corresponds to the magnitude of an earthquake. To the left (i.e. backward in time) of each peak is one peak (the trigger) and to the right (i.e. forward in time) of each peak may be several (the direct aftershocks), connected from left to right via a ridge linking trigger to offspring. Since the height of the peaks varies (according to the GR law), some of the peaks will be below water (below the detection threshold). A whole part of the branch may be submerged in water (i.e. unobserved) until eventually a peak rises above the surface and appears to have no ridge connecting it to a previous peak, because the ridge of the last observable mountain simply descends into the water.

This view leads to the conclusion that the average number of direct aftershocks that are observed will be less than the real branching ratio, since some of the triggered events of an observed shock will fall below m_d and hence not be included in the count. Only the fraction f_{obs} from equation (7) above m_d of the total direct aftershocks $\rho(m)$ will be observed. Moreover, the pdf $P(m|m \geq m_d)$ of mother events conditioned on being larger than m_d is zero for $m < m_d$ and equal to $P(m)/f_{obs}$ for $m_{max} > m \geq m_d$. We can thus define the apparent branching ratio as

$$\begin{aligned} n_a &\equiv \int_{m_0}^{m_{max}} P(m|m \geq m_d)\rho(m)f_{obs}dm \\ &= \int_{m_d}^{m_{max}} P(m)\rho(m)dm \\ &= \frac{kb}{b-\alpha} \left(\frac{10^{-(b-\alpha)(m_d-m_0)} - 10^{-(b-\alpha)(m_{max}-m_0)}}{1 - 10^{-b(m_{max}-m_0)}} \right) \end{aligned} \quad (10)$$

for the case $\alpha \neq b$. The special case $\alpha = b$ gives

$$n_a = \frac{kb \ln(10)(m_{max} - m_d)}{1 - 10^{-b(m_{max} - m_0)}}. \quad (11)$$

Using equation (4) and eliminating k , we have n_a in terms of n :

$$n_a = n \left(\frac{10^{(b-\alpha)(m_{max} - m_d)} - 1}{10^{(b-\alpha)(m_{max} - m_0)} - 1} \right), \quad (12)$$

when $\alpha \neq b$, and

$$n_a = n \left(\frac{m_{max} - m_d}{m_{max} - m_0} \right), \quad (13)$$

when $\alpha = b$.

According to expression (12), $n_a \leq n$, where the equality holds for m_d equal to m_0 . In principle, equation (12) also holds for $n > 1$, but we restrict this study to the stationary regime $n < 1$. Figure 2 shows n_a as a function of n for a range of values of m_0 for the case $\alpha = b$. The values of m_0 are $m_0 = m_d = 3$ (solid), $m_0 = 0$ (dashed), $m_0 = -5$ (dotted) and $m_0 = -10$ (dash-dotted). We assumed $m_d = 3$ and $m_{max} = 8$. Specifying m_0 then fixes the linear slope of the dependence between n and n_a . Figure 2 demonstrates that the apparent (measurable) fraction of aftershocks may significantly underestimate the true fraction of aftershocks even for m_0 not very small. For example, $m_0 = -5$ roughly translates a real branching ratio of $n = 0.9$ into an apparent branching ratio $n_a = 0.3$. Decreasing α below b places more importance on the triggering from small earthquakes and therefore strongly amplifies this effect.

In Figure 3, we plot the ratio n_a/n as a function of the unknown m_0 . Again, we assume $m_d = 3$, $m_{max} = 8$, $b = 1$, but now we let $\alpha = 0.5$ (dash-dotted), $\alpha = 0.8$ (dashed) and $\alpha = b = 1.0$ (solid). As expected, when $m_0 = m_d$, the ratio is one because there is no unobserved seismicity. As m_0 goes to minus infinity, n_a approaches zero since almost all seismicity occurs below the threshold. We see clearly that unobserved seismicity results in a drastic underestimate of the fraction of aftershocks.

Given an estimate of the magnitude of the smallest triggering earthquake m_0 (see *Sornette and Werner* [2004] and references therein), one can calculate the true branching ratio from the apparent branching ratio. In fact, *Sornette and Werner* [2004] obtained four estimates of m_0 as a function of n by comparing the ETAS model prediction of the number of observed aftershocks (8) from fits to observed aftershock sequences and from the empirical Båth's law. Their equations (10), (13), (16) and (18) are the estimates of m_0 as a function of n and a number of known constants specific to the fits to observed aftershock sequences. We can use these relations of m_0 as a function of n to eliminate m_0 from equation (12) to obtain direct estimates of n as a function of the measurable n_a . For simplicity, we restrict the use of their findings to the case $\alpha = b$. The estimate resulting from the fits performed by *Helmstetter et al.* [2004] yielded

$$m_0 = m_{max} - \left(\frac{n}{1-n} \right) \frac{\theta c^\theta}{K_{fit}} \frac{1 - 10^{-b(m_{max} - m_d)}}{b \ln(10)} \quad (14)$$

with the values $m_{max} = 8.5$, $m_d = 3$, $\theta = 0.1$, $c = 0.001$, $b = 1$ and $K_{fit} = 0.008$. The study initiated by *Felzer et al.* [2002] provided another estimate

$$m_0 = m_{max} - \frac{n}{1-n} \frac{(1 - 10^{-b(m_{max} - m_d)})}{b \ln(10)} \times \frac{\theta_T c^{\theta_T}}{A_T} 10^{b(M_1 - m_d)}, \quad (15)$$

where $m_{max} = 8.5$, $m_d = 3$, $\theta_T = 0.08$, $A_T = 0.116$ days $^{-\theta_T}$, $b = \alpha = 1$, $c = 0.014$ and $M_1 = 6.04$. Using the declustering performed by *Reasenber and Jones* [1989], *Sornette and Werner* [2004] obtained

$$m_0 = m_{max} - \frac{n}{1-n} \frac{\theta c^\theta 10^{-a}}{b \ln(10)} (1 - 10^{-b(m_{max} - m_d)}) \quad (16)$$

where $m_{max} = 8.5$, $m_d = 3$, $\theta = 0.08$, $a = -1.67$, $c = 0.05$ and $b = 1$. Finally, using Båth's law, *Sornette and Werner* [2004] found

$$m_0 = m_{max} - \left(\frac{n}{1-n} \right) \frac{(1 - 10^{-b(m_{max} - m_d)})}{b \ln(10)} 10^{b(M_1 - m_a)} \quad (17)$$

where $M_1 - m_a = 1.2$ according to the the law, $b = 1$, $m_{max} = 8.5$, and $m_d = 3$.

Substituting these four estimates of m_0 from equations (14), (15), (16), and (17) into equation (12) for n_a provides four estimates of n_a versus n all in terms of known constants. These four estimates of n as a function of n_a can be used to find the correct fraction of aftershocks from the measurable apparent fraction of aftershocks. Figure 4 shows these four estimates with the above constants. As noted above, n varies linearly with n_a with a slope determined by m_0 . The four estimates of n as a function of n_a allow for all possible values of m_0 . The solid line $n = n_a$, corresponding to the slope 1 when $m_0 = m_d$, separates the left side of the graph, where $m_0 < m_d$, from the right side, where $m_0 \geq m_d$, which can be ruled out based on observed aftershocks from magnitudes 2. Thus, only the region to the left of the diagonal should be considered.

Figure 4 can be used to find the real fraction of aftershocks from the measured apparent fraction by assuming one of the four estimates of m_0 as a function of n . For example, *Helmstetter et al.* [2004] find that 55 percent of all earthquakes are aftershocks above $m_d = 3$. Using their values to estimate m_0 as a function of n , we can determine that the real fraction of aftershocks is closer to 75 percent. Thus the size of this effect is significant. Furthermore, having determined a point on the line estimating n from n_a for all values of m_0 fixes the slope of $n(n_a)$ and therefore m_0 . Using their values, we find $m_0 = 1.2$. Similar estimates can be made using the apparent fraction of aftershock values found by *Felzer et al.* [2002] and *Reasenber and Jones* [1989].

Assuming that current maximum likelihood estimation methods of the ETAS model parameters, which assume $m_0 = m_d$, determine a branching ratio that corresponds to the present apparent branching ratio, we can similarly correct these values to find the true fraction of aftershocks using Figure 4. For example, *Zhuang et al.* [2004] find a "criticality parameter" of about 45 percent, which we take as a proxy for n_a . Figure 4 shows that the true branching ratio then lies between 0.45 and 0.80, depending on which estimate (among the four models (14), (15), (16), and (17)) of m_0 as a function of n is chosen. These calculations suggest that previous estimates of the fraction of aftershocks obtained by various declustering methods significantly underestimated its value.

3.2. Determination of apparent background events S_a of uncorrelated seismicity

In order to derive the number of shocks within one cascade that are not triggered by a mother above the threshold and thus appear as independent background events, we need to distinguish between the case where the initial (main)

shock of magnitude M_1 is observable (i.e. $M_1 \geq m_d$) and the case where it is undetected (i.e. $M_1 < m_d$).

If $M_1 \geq m_d$, then the initial mainshock produces $\rho(M_1)f_{obs}$ observed direct aftershocks. On average, these will in turn collectively produce $\rho(M_1)f_{obs}n_a$ observed second generation aftershocks. We specifically do not consider events above m_d triggered from below m_d , which we deal with below in the definition of the apparent background sources. By continuing this ‘‘above-water’’ cascade for all generations of aftershocks, we can calculate the number of triggered events that are in direct lineage above the threshold back to the mainshock as the infinite sum of terms of $\rho(M_1)f_{obs}$ multiplied by the apparent branching ratio n_a to the power of the generation. If, on the other hand, the initial mainshock is below m_d , then no such direct ‘‘above-water’’ cascade will be seen. Any observed shock will be triggered by an event below the water. Thus, for the two cases, the ‘‘above-water’’ sequence is expressed as:

$$N_{above} = \begin{cases} \frac{\rho(M_1)f_{obs}}{1-n_a} = N_{obs} \frac{1-n}{1-n_a} & , M_1 \geq m_d \\ 0 & , M_1 < m_d \end{cases} \quad (18)$$

Furthermore, since in the ETAS model, a small earthquake may trigger large earthquakes, an event below m_d may produce an observed event above m_d . An inversion method that reconstructs the entire branching structure of the model from an earthquake catalog will identify these shocks as background events. But since in reality these events were triggered by earthquakes below the detection threshold, we will refer to them as apparent background events. These events can of course trigger their own cascades. We thus define apparent background source S_a as the number of observed events above m_d that are apparently not triggered, i.e. have ‘‘mothers’’ below m_d . Again, we distinguish between the cases where the mainshock magnitude is $M_1 \geq m_d$ and $M_1 < m_d$. For the first, S_a is given by the total number of aftershocks below the threshold multiplied by the average number r of direct aftershocks they trigger above the threshold. For the second case, we must also include the direct aftershocks of the initial mainshock that are observed:

$$S_a = \begin{cases} \frac{\rho(M_1)}{1-n} (1-f_{obs})r & , M_1 \geq m_d \\ \frac{\rho(M_1)}{1-n} (1-f_{obs})r + \rho(M_1)f_{obs} & , M_1 < m_d \end{cases} \quad (19)$$

Now, the number r of observable direct aftershocks above m_d averaged over unobserved mothers between m_0 and m_d is given by the following conditional branching ratio:

$$r \equiv \int_{m_0}^{m_d} P(m|m < m_d) \rho(m) f_{obs} dm \quad (20)$$

$$= (n - n_a) \left(\frac{f_{obs}}{1 - f_{obs}} \right), \quad (21)$$

where we have used $P(m|m < m_d) = P(m)/(1 - f_{obs})$ for $m < m_d$ and zero otherwise. Substituting (21) into the expression for the apparent source (19) and re-arranging using (8), we obtain

$$S_a = \begin{cases} \frac{\rho(M_1)}{1-n} f_{obs} (n - n_a) & , M_1 \geq m_d \\ \frac{\rho(M_1)}{1-n} f_{obs} (n - n_a) + \rho(M_1) f_{obs} & , M_1 < m_d \end{cases} \\ = \begin{cases} N_{obs} (n - n_a) & , M_1 \geq m_d \\ N_{obs} (n - n_a) + \rho(M_1) f_{obs} & , M_1 < m_d \end{cases} \quad (22)$$

Equation (22) shows that, for each genuine background event, a perfect inversion method would count S_a apparent background events. Figure 5 plots the number of apparent background events S_a as a function of the branching ratio

n for an example aftershock cascade set off by a magnitude $m = 5$ initial shock. We assumed the values $m_{max} = 8.5$, $m_d = 3$ and $\alpha = b = 1.0$. The figure shows that for one cascade, i.e. one independent background event, hundreds of earthquakes appear as apparent background events when $m_0 < m_d$.

In Figure 6, we investigate the relative importance of the apparent background events with respect to the observed number of aftershocks of one cascade. According to equation (22)

$$S_a/N_{obs} = n - n_a, \quad (23)$$

i.e. a significant fraction $n - n_a$ of events of the actually observed aftershocks are falsely identified as background events (since all events are really triggered from a single mainshock in our example). For $m_d = m_0$, the ratio is zero, since no events trigger below the detection threshold. However, as m_0 decreases and more and more events fall below m_d , the fraction increases until n_a goes to zero and the ratio approaches n . This effect increases with decreasing α . Small values of α generally place more importance on the cumulative triggering of small earthquakes.

3.3. Consistency check: N_{obs} as the sum of ‘‘above-water’’ cascades triggered by the mainshock and by the apparent background events

To complete the calculations and show consistency of the results, we now demonstrate that the observed cascades set off by the apparent background events, when added to the original ‘‘above-water’’ cascade, add up to the total observed number of aftershocks of the whole sequence. Each apparent source event will trigger its own cascade above the threshold m_d with branching ratio n_a . The total number of events due to the apparent background events and their cascades above the threshold is

$$N_{source} = S_a + S_a n_a + S_a n_a^2 + \dots = \frac{S_a}{1 - n_a}. \quad (24)$$

Substituting expression (22) and using (8) gives

$$N_{source} = \begin{cases} N_{obs} \frac{(n-n_a)}{1-n_a} & , M_1 \geq m_d \\ N_{obs} \frac{(n-n_a)}{1-n_a} + \frac{\rho(M_1-m_0)f_{obs}}{1-n_a} & , M_1 < m_d \end{cases} \quad (25)$$

Combining the direct ‘‘above-water’’ cascade (18) with the apparent source cascades (25) gives the total amount of apparent events observed after the initial event

$$N_a = N_{source} + N_{above} \\ = \begin{cases} N_{obs} \frac{(n-n_a)}{1-n_a} + \frac{\rho(M_1-m_0)f_{obs}}{1-n_a} & , M_1 \geq m_d \\ N_{obs} \frac{(n-n_a)}{1-n_a} + \frac{\rho(M_1-m_0)f_{obs}}{1-n_a} + 0 & , M_1 < m_d \end{cases} \\ = N_{obs}, \quad (26)$$

where N_{obs} is given by (8). The last equality confirms the consistency of our decomposition into apparently-triggered earthquakes and apparent sources.

Expressions (10) and (22) show that analyzing the tree structure of triggered seismicity only above the detection threshold leads to the introduction of an apparent source S_a and an apparent branching ratio n_a . It is important to realize that both are renormalized simultaneously by $m_d \neq m_0$. If the current inversion techniques for the ETAS parameters were perfect and correctly reconstructed the tree structure of all sequences, the inverted values would be equal to our analytical results (10) and (22). Accordingly, the value of the background source would be overestimated and the branching ratio underestimated. In fact, one single true sequence will appear as many different sequences, each apparently set off by an apparent background event.

4. Conclusions

We have shown that unbiased estimates of the fraction of aftershocks and the number of independent background events are simultaneously renormalized to apparent values when the smallest triggering earthquake m_0 is smaller than the detection threshold m_d . In summary, mainshocks above the threshold will appear to have less aftershocks, resulting in a smaller apparent branching ratio. Meanwhile, unobserved events can trigger events above the threshold giving rise to apparently independent background events that seem to increase the constant background rate to an apparent rate. Assuming that current techniques which are used to invert for the parameters of the ETAS model (for example, the maximum likelihood method) under the assumption $m_d = m_0$ are unbiased estimators of n_a and S_a , then the obtained values for the fraction of aftershocks and the background source rate correspond to renormalized values because of the assumption that the detection threshold m_d equals the smallest triggering earthquake m_0 . We predict that n will be drastically underestimated and S strongly overestimated for m_0 much smaller than m_d .

Acknowledgments. We acknowledge useful discussions with A. Helmstetter and J. Zhuang. This work is partially supported by NSF-EAR02-30429, and by the Southern California Earthquake Center (SCEC). SCEC is funded by NSF Cooperative Agreement EAR-0106924 and USGS Cooperative Agreement 02HQAG0008. The SCEC contribution number for this paper is xxx. MJW gratefully acknowledges financial support from a NASA Earth System Science Graduate Student Fellowship.

References

- Athreya, K. B. and P. E. Ney (1972), *Branching Processes*, Springer Verlag, Berlin, Germany.
- Console, R., M. Murru, and A. M. Lombardi (2002), Refining earthquake clustering models, *J. Geophys. Res.*, 108(B10), 2468, doi:10.1029/2002JB002123.
- Felzer, K. R., T. W. Becker, R. E. Abercrombie, G. Ekström, and J. R. Rice (2002), Triggering of the 1999 M_W 7.1 Hector Mine earthquake by aftershocks of the 1992 M_W 7.3 Landers earthquake, *J. Geophys. Res.*, 107(B9), 2190, doi:10.1029/2001JB000911.
- Helmstetter, A. (2003), Is earthquake triggering driven by small earthquakes?, *Phys. Rev. Lett.* 91, 10.1103/PhysRevLett.91.058501.
- Helmstetter, A., Y. Y. Kagan, and D. D. Jackson (2004), Importance of small earthquakes for stress transfers and earthquake triggering, *J. Geophys. Res.*, submitted.
- Helmstetter, A., and D. Sornette (2002), Subcritical and supercritical regimes in epidemic models of earthquake aftershocks, *J. Geophys. Res.*, 107(B10), 2237, doi:10.1029/2001JB001580.
- Helmstetter, A. and D. Sornette (2003), Foreshocks explained by cascades of triggered seismicity, *J. Geophys. Res.* 108 (B10), 2457 10.1029/2003JB002409 01.
- Helmstetter, A., and D. Sornette, (2003), Importance of direct and indirect triggered seismicity in the ETAS model of seismicity, *Geophys. Res. Lett.*, 30(11), 1576, doi:10.1029/2003GL017670.
- Kagan, Y.Y. (1991), Likelihood analysis of earthquake catalogs, *Geophys. J. Int.* 106, 135-148.
- Kagan, Y. Y. (1999), Universality of the seismic moment-frequency relation, *Pure and Appl. Geophys.* 155, 537-573.
- Kagan, Y.Y. (2003), Accuracy of modern global earthquake catalogs, *Phys. Earth Plan. Inter.* 135, 173-209.
- Kagan, Y. Y., and L. Knopoff (1981), Stochastic synthesis of earthquake catalogs, *J. Geophys. Res.*, 86, 2853-2862.
- Nechad, H., A. Helmstetter, R. El Guerjouma and D. Sornette (2004), Andrade and critical time-to-failure laws in fiber-matrix composites: Experiments and model, in press in *Journal of Mechanics and Physics of Solids (JMPS)* (<http://arXiv.org/abs/cond-mat/0404035>)
- Ogata, Y. (1988), Statistical models for earthquake occurrence and residual analysis for point processes, *J. Am. Stat. Assoc.*, 83, 9-27.
- Ogata, Y. (1998), Space-time point-process models for earthquake occurrence, *Ann. Inst. Statist. Math.*, Vol. 50, No. 2, 379-402.
- Ouillon, G. and D. Sornette (2004), Magnitude-dependent Omori law: Theory and empirical study, in press in *J. Geophys. Res.* (<http://arXiv.org/abs/cond-mat/0407208>).
- Sellers, E. J., M. O. Kataka, and L. M. Linzer (2003), Source parameters of acoustic emission events and scaling with mining-induced seismicity, *J. Geophys. Res.*, 108(B9), 2418, doi:10.1029/2001JB000670.
- Sornette, D., and A. Helmstetter (2002), Occurrence of finite-time singularities in epidemic models of rupture, earthquakes and starquakes, *Phys. Rev. Lett.* Vol. 89, No. 15, 158,501.
- Sornette, D. and M. J. Werner (2004), Constraints on the Size of the Smallest Triggering Earthquake from the ETAS Model, Bath's Law, and Observed Aftershock Sequences, *J. Geophys. Res.*, submitted. (<http://www.arxiv.org/abs/physics/0411114>)
- Utsu, T., Y. Ogata, and R. S. Matsu'ura (1995), The centenary of the Omori formula for a decay law of aftershock activity, *J. Phys. Earth*, 43, 1-33.
- Zhuang, J., Y. Ogata, and D. Vere-Jones (2004), Analyzing earthquake clustering features by using stochastic reconstruction, *J. Geophys. Res.* 109, B05301, doi:10.1029/2003JB002879.

D. Sornette, Department of Earth and Space Sciences, and Institute of Geophysics and Planetary Physics, University of California, Los Angeles, California 90095, USA and Laboratoire de Physique de la Matière Condensée, CNRS UMR6622, Université de Nice-Sophia Antipolis, Parc Valrose, 06108 Nice Cedex 2, France. (sornette@moho.ess.ucla.edu)

M. J. Werner, Department of Earth and Space Sciences, and Institute of Geophysics and Planetary Physics, University of California, Los Angeles, California 90095, USA. (werner@moho.ess.ucla.edu)

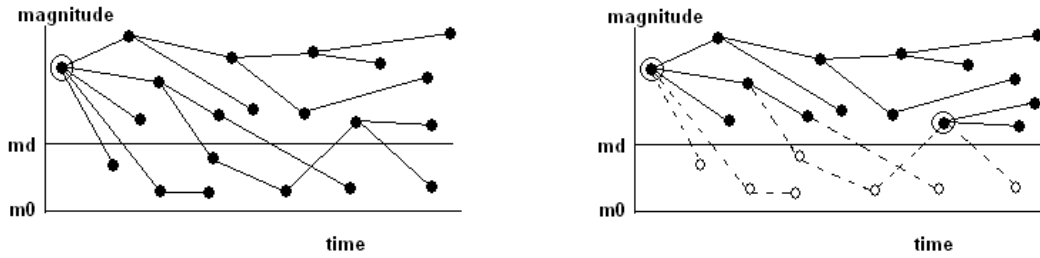


Figure 1. Schematic representations of the branching structure of the real ETAS model (left) and the apparent ETAS model (right). The initial mainshock is circled. Only events above the detection threshold m_d are observed. The apparent branching ratio does not take into account unobserved triggered events (dashed lines). An observed event triggered by a mother below m_d appears as an untriggered background source event (circled).

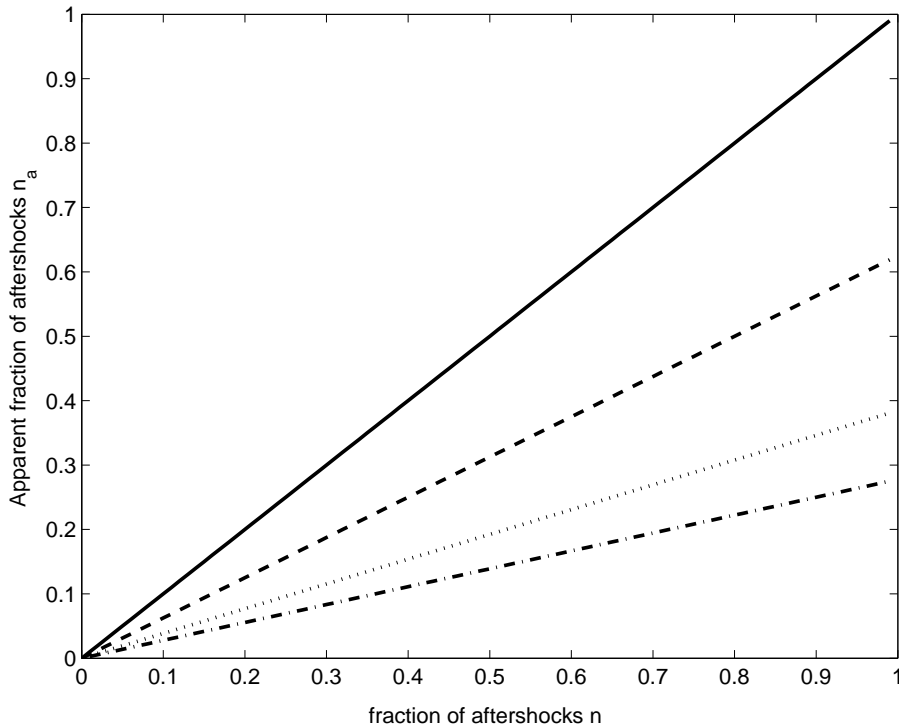


Figure 2. The apparent fraction of aftershocks (apparent branching ratio) n_a varies linearly with the real fraction of aftershocks (real branching ratio) n with a slope fixed by the smallest triggering earthquake m_0 . As m_0 decreases, the apparent fraction of aftershocks significantly underestimates the real fraction. As examples, we chose $m_0 = m_d = 3$ (solid), i.e. $n_a = n$ and no events are missed; $m_0 = 0$ (dashed); $m_0 = -5$ (dotted); and $m_0 = -10$ (dash-dotted). We further assumed parameters $m_d = 3$, $m_{max} = 8$, $b = 1$, and $\alpha = 1.0$. A small value of α amplifies this effect (see Figure 3).

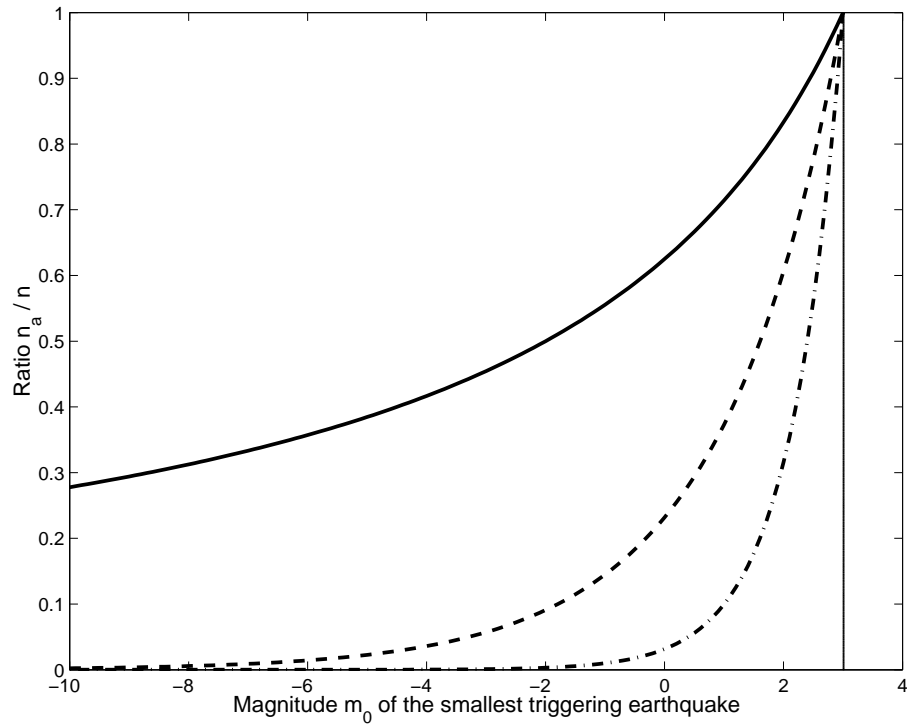


Figure 3. The ratio of the apparent fraction of aftershocks (apparent branching ratio) n_a over the real fraction of aftershocks (real branching ratio) n varies as a function of the smallest triggering earthquake m_0 . For $m_0 = m_d$, $n_a = n$ and all events are detected above the threshold. For a small value of m_0 , the ratio becomes small, indicating that n_a significantly underestimates n . Decreasing α amplifies this effect. We used parameters $m_d = 3$ (vertical reference line), $m_{max} = 8$, $b = 1$. We varied $\alpha = 0.5$ (dash-dotted), $\alpha = 0.8$ (dashed), $\alpha = 1.0$ (solid).

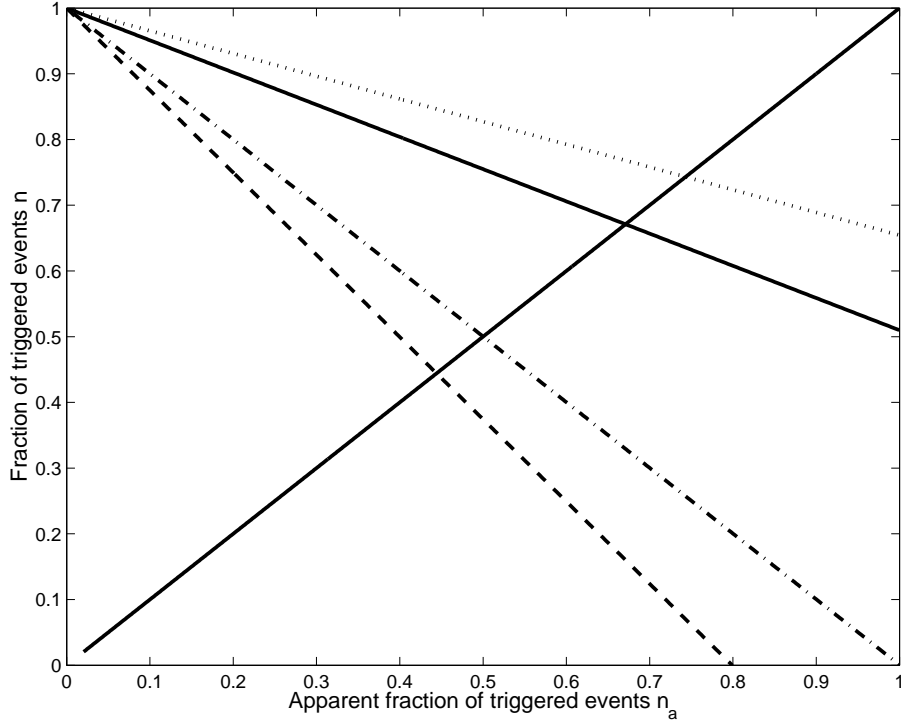


Figure 4. The fraction of aftershocks (branching ratio) n can be estimated from the apparent fraction of aftershocks (apparent branching ratio) n_a by using four estimates of the smallest triggering earthquake m_0 as a function of n as determined in *Sornette and Werner* [2004] (see text). The estimates of m_0 as a function of n were obtained from comparisons of the ETAS model prediction of the number of observed aftershocks and fits to observed aftershock sequences performed by *Helmstetter et al.* [2004] (solid), *Felzer et al.* [2002] (dash-dotted), *Reasenberg and Jones* [1989] (dotted) and from Bath's law (dashed). The additional diagonal solid line $n_a = n$ corresponds to $m_0 = m_d$ (no undetected events). Along any of the four lines, m_0 varies from minus infinity to m_{max} . Given that we can rule out $m_0 \geq m_d$, we can restrict the physical range to the left side of the reference curve $n_a = n$. Given an estimate of the apparent (measured) fraction of aftershocks n_a , we can estimate the real fraction from one of the four lines. Because n is linearly proportional to n_a , an estimate of n_a not only determines n from one of the curves, but also estimates m_0 from the slope of the line connecting the point (n_a, n) to the origin. For example, the estimate of *Helmstetter et al.* [2004] of 55 percent of observed aftershocks approximately gives a real fraction n of 75 percent according to their own fits to aftershocks and thereby determines $m_0 = 1.2$ for $m_{max} = 8$ and $m_d = 3$.

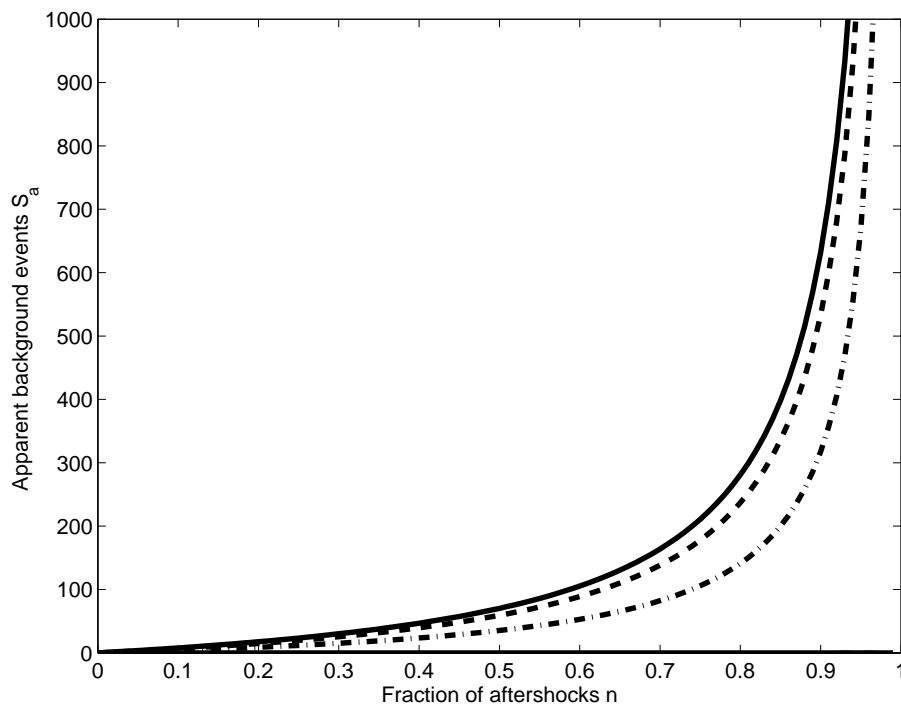


Figure 5. The number of apparent background events S_a in an aftershock cascade due to a single background event of magnitude $M_1 = 5$ as a function of the fraction of aftershocks (branching ratio) n for several values of the smallest triggering earthquake. For $m_0 = m_d$, no events are missed. Therefore the number of apparent background events is zero. As m_0 decreases, events below the detection threshold trigger events above the threshold and hence the number of apparent background events increases. We vary $m_0 = m_d = 3$ (solid, coinciding with x-axis), $m_0 = 0$ (dash-dotted), $m_0 = -5$ (dashed), and $m_0 = -10$ (upper solid curve). We used parameters $m_d = 3$, $m_{max} = 8$, $b = 1$, and $\alpha = 1.0$. For very small m_0 and n close to 1, almost all events above the detection threshold are triggered from below and thus S_a becomes very large (see Figure 6). This effect is amplified for decreasing α (not shown).

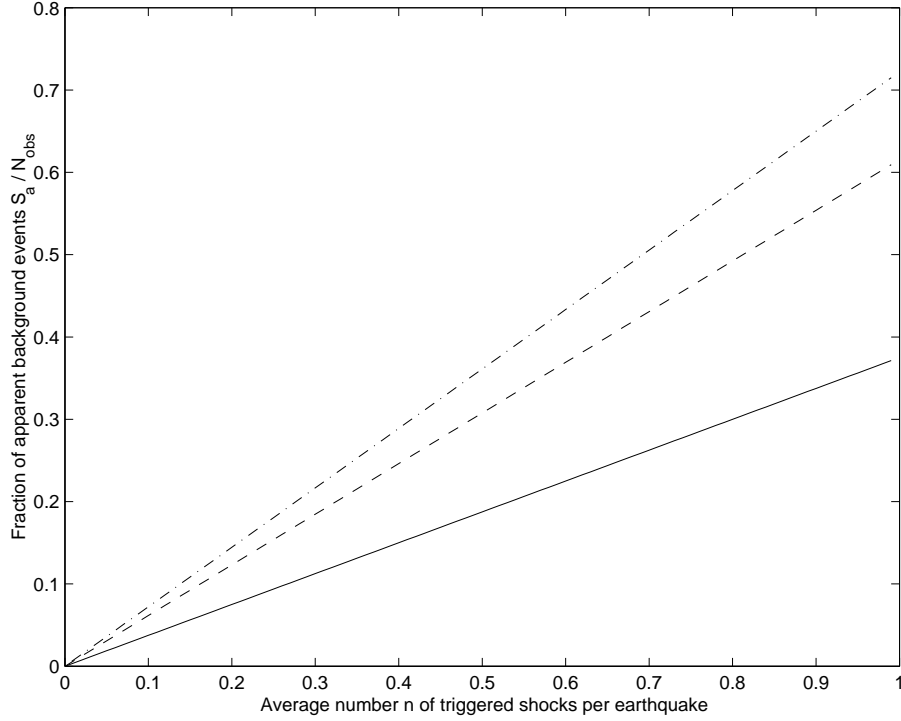


Figure 6. The ratio of the number of apparent background events S_a over the total observed number N_{obs} of aftershocks of one cascade varies as $n - n_a$. Here, we show the ratio as a function of the branching ratio n by assuming a particular value of m_0 . For $m_0 = m_d$ (solid, coinciding with x-axis), there are no apparent background sources. For m_0 less than m_d , the ratio increases as more and more of the observed events are triggered by unobserved events. As examples, we show the ratio S_a/N_{obs} for $m_0 = m_d = 3$ (solid, coinciding with x-axis), $m_0 = 0$ (upper solid line), $m_0 = -5$ (dashed) and $m_0 = -10$ (dash-dotted) as a function of the branching ratio n (average number of aftershocks per earthquake also equal to the fraction of aftershocks in a catalog) for parameters $m_d = 3$, $m_{max} = 8$, $b = 1$, and $\alpha = 1.0$. For very small m_0 , n_a approaches zero and the ratio S_a/N_{obs} approaches its limiting value n , meaning that almost all observed earthquakes were triggered by events below the detection threshold m_d . The effect of unobserved events triggering observed quakes resulting in an apparent background source rate is further amplified by smaller values of α (not shown).